Available online at www.sciencedirect.com

SCIENCE DIRECT®

Journal of Photochemistry and Photobiology A: Chemistry 167 (2004) 49–57

Journal of Photochemistry and Photobiology A:Chemistry

www.elsevier.com/locate/jphotochem

Effect of alkaline-doped TiO_2 on photocatalytic efficiency

Y. Bessekhouad, D. Robert*, J-V Weber, N. Chaoui

Laboratoire de Chimie et Applications (EA 3471), Université de Metz, Rue Victor Demange, 57500 Saint-Avold, France

Received 13 November 2003; received in revised form 13 November 2003; accepted 2 December 2003

Available online 20 June 2004

Abstract

Alkaline (Li, Na, K) modified titanium dioxide nanoparticles were prepared by sol–gel route and by impregnation technology. XRD analysis showed that the crystallinity level of catalysts is largely dependent on both the nature and the concentration of alkaline. Indeed, the best crystallinity is obtained for Li-doped TiO_2 and is lowest for K-doped TiO_2. In general, it was found that the anatase phase is stabilised by the alkaline. pH of zero charge has been found to be in the range 6.6–7.9. Depending on the alkaline concentration, the charge compensation may occur at the surface of the catalyst in acidic and basic environment. For photocatalytic test, Malachite green oxalate, 4-hydroxybenzoic acid and benzamide were used as representative organic pollutants. The catalysts prepared by the impregnation technique were found more efficient than those prepared by sol–gel route, for a given alkaline concentration. When applied to the Malachite green degradation, the best results were obtained for 5% Li-doped TiO_2 prepared by impregnation technique. Whatever the alkaline used, and at low concentration, our results show that the efficiency of the catalysts, when prepared by impregnation technique, is better than that of TiO_2-P25. Therefore, at low concentration, alkaline doped-TiO_2 can be considered as promising materials for organic pollutants degradation.

© 2003 Elsevier B.V. All rights reserved.

Keywords: Titanium dioxide; Lithium; Sodium; Potassium; Photocatalysis; Sol–gel route; Nanosized particle; Doping

1. Introduction

In recent years, the photocatalytic decomposition of organic pollutants in water has received much attention [1–8]. These reactions are of particular interest due to their ability to use the solar energy. TiO_2 is the most popular semiconductor used in photocatalytic processes [1–8]. Large crystallites of pure TiO_2 size are stoechiometric and thus show poor activity when applied in photocatalysis. However, nanometer-sized TiO_2 crystallites (typical size <50 nm) present Ti deficiency and fulfil the expected electronical properties for applications in photocatalysis.

TiO_2 can be used both pure or doped with metals or metal oxides. These modifications can enhance its photocatalytic activity. The dominant parameters include the nature, the concentration of dopant, and the thermal treatment of the material [9]. Brezová et al. [9] reported that the presence of metals, such as Li^+, Zn^{2+}, Cd^{2+}, Pt^0, Ce^{3+}, Mn^{2+}, Al^{3+} and Fe^{3+}, may significantly change the photoactivity of TiO_2 prepared by sol–gel technique. These authors showed that doping TiO_2 with Li^+, Zn^{2+} or Cd^{2+} improves the photoactivity of TiO_2 [9] with the maximum effect of Li^+ in the case of phenol photodecomposition. The effect of doping TiO_2 with Li and Rb was also studied by López et al. [10]. The obtained materials, nanocrystallite sol–gel derived catalysts, were used for the decomposition of 2,4-dinitroaniline. The obtained results showed an inhibition of activity that was attributed to the presence of Li in TiO_2 network. Indeed, Li can act as an electron trap when it is as Li–O or hole trap when it is as Li^0. These two examples illustrate the difficulty to explain the influence of metal doping on the activity of the TiO_2.

Morawski et al. [11] reported the preparation of K-doped TiO_2 by impregnation technology. KNO_3, K_2CO_3, KOH and metallic potassium were used for the preparation of the catalysts. Phenol was used as a model pollutant to study the efficiency of catalysts. TiO_2/KNO_3, TiO_2/K_2CO_3 and TiO_2/KOH were reported to be inactive on phenol photocatalytic decompositions. However, using elemental potassium K^0 as a raw material in the preparation procedure of K-doped TiO_2 leads to a more active catalyst than pure TiO_2. The so-obtained material forms a mixture of TiO_2 with $K_2Ti_4O_9$ (perovskite structure) and a phase including potassium that is probably in lamellar host. The authors attributed the activation of catalyst to a more efficient electron–hole creation induced by the presence of potassium. These results are in sharp opposition to those obtained by Grzechulska et al. [12]

---

* Corresponding author. Tel.: +33-387939108; fax: +33-387939101.
E-mail address: drobert@iut.univ-metz.fr (D. Robert).

1010-6030/$ – see front matter © 2003 Elsevier B.V. All rights reserved.
doi:10.1016/j.jphotochem.2003.12.001

who reported the high abilities of TiO_2/KOH to decompose oil dispersed in water. The catalyst consisted of a complex mixture of various titanium oxides that are thought to be responsible for the activity increase.

On the other hand, it may occur that the alkaline contamination of TiO_2 results from an unavoidable step in a preparative procedure. As an example, during the preparation of glass supported TiO_2, some authors observed Na^+ migration from the support to the TiO_2 layers during a necessary thermal treatment step [13,14]. Consequently, Na^+, present in the titania lattice, acts as electron–hole trapping centre and according to these authors, this phenomenon is responsible for the decrease in the photoactivity of the supported materials.

From the work of these authors, it clearly appears that the effect of individual metal ions on the photocatalytic activity of doped-TiO_2 is a complex problem that depends not only on the dopant nature but also on the preparative procedure of the materials and the pollutant to degrade.

The aim of this work is to clarify the effect of the preparative procedure and the amount of alkaline dopant on photocatalytic activity of TiO_2. For that purpose, alkaline-doped TiO_2 at different concentrations was prepared by two methods: sol–gel route and impregnation technology. The prepared samples were characterized by means of XRD in order to identify the obtained phase(s) and the crystallite size. The pH drift method has been used in order to measure the acidobasic properties of the surface. The photocatalytic activity of the prepared samples has been evaluated for the degradation of a set of representative pollutants: Malachite green oxalate as a dye, 4-hydroxybenzoic acid as a representative for organic acids and benzamide as an organic base. The effects of the concentration of each alkaline versus the degradation of each kind of organic pollutant are analysed and discussed.

2. Experimental

2.1. Catalysts preparation

The following commercial reagents were used without any further purification: tetraisopropylorthotitanate $Ti(OC_3H_7)_4$ (Aldrich, 97%), $LiNO_3$ (Aldrich, 99.9%), $NaNO_3$ (Aldrich, 99.9%), KNO_3 (Aldrich, 99.9%), ethanol (SdS-France, 99.9%), methanol (SdS-France, 99.9%), TiO_2 P25 (Degussa), Malachite green oxalate (Reactifs RAL. France), 4-hydroxy benzoic acid (Aldrich, 99%), benzamide (Aldrich, 99%).

For the catalyst preparation, the following methods have been adopted:

1. Direct method: $Ti(OC_3H_7)_4$ solution is dissolved in methanol/ethanol with molar ratio 1:1:10 and heated during 3 h (bath temperature = 75 °C). An appropriate amount of water is added drop-wise into the hot solution (75 °C) [15]. In such case the water contained dissolved ANO_3 (A: Li, Na, K) and the amount of A^+ was varied from 1 to 5% relatively to Ti^{4+}. After gelling, the samples were dried at 110 °C for 12 h and then heat-treated in air for 10 h at 550 °C with a heating rate of 3 °C/min. The resulting products are labelled x%A–TiO_2 d ($x = 0, 1, 3, 5$ and d: direct).
2. Impregnation method: pure TiO_2 resulting from the sol–gel method, described below, is dispersed in solution containing appropriate molar concentration of A^+. The solution is agitated for 1 h after 15 min of sonication and then dried at 110 °C during 12 h. After homogenisation by grounding in a mortar, the powder is calcinated at 400 °C for 1 h with a heating rate of 3 °C/min. The samples resulting from this method are labelled x%A–TiO_2 i ($x = 1, 3, 5$ and i: impregnation).

2.2. Sample characterizations

X-ray diffraction (XRD) patterns were collected at 295 K using Cu Kα ($\lambda = 0.15418$ nm) radiation and were used to identify the phases in presence and their crystallite sizes. The average crystalline sizes of anatase and rutile were determined according to the Scherrer equation using the full-width at half-maximum (FWHM) of the peak presenting the highest intensity and taking into account the instrument broading.

The pH of the point of zero charge pH_{pzc} was measured by the so-called pH drift method [16]. For this purpose, 500 ml of a 0.01 M NaCl solution were degassed using N_2 in order to eliminate and prevent further dissolution of carbon dioxide. From this preliminary solution, five solutions with pH ranging from 3 to 12 were prepared (by adding either HCl or NaOH). Ten milligram of catalyst were added into 10 ml of each solution. The final pH (reached after 24 h) was measured and plotted as a function of initial pH. The pH at which the curve crosses the line pH (final) = pH (initial) is the pH_{pzc} of the given catalyst.

2.3. Photocatalytic experiments

Photocatalytic activity of prepared catalysts was taken as its ability to degrade malachite green, 4-hydroxybenzoic acid and benzamide. A Solar box ATLAS Suntest CPS+ simulating natural radiation equipped with Xenon lamp was used in all experiments. When malachite green (MG) was used as a pollutant, 125 mg of catalyst were dissolved in 250 ml of MG (10 mg/l) solution. Before irradiation, the mixture was sonicated for 2 min in order to disperse the catalysts and then maintained in dark for 1 h. At given irradiation time intervals, 5 ml of the solution were taken and analyzed by means of a UV-Vis spectrophotometer (Shimadzu PC1201, maximum absorbance was taken at 618 nm).

The remaining concentration of 4-hydroxybenzoic acid and benzamide was followed by HPLC equipped with a C18 column. One hundred and twenty-five milligram of each catalyst were dispersed in 250 ml of solution containing either 20 mg/l of benzamide or 30 mg/l of 4-hydroxybenzoic acid and sonicated for 2 min before irradiation. During the photocatalytic degradation, 10 ml of solution were regularly taken, filtered (Whatmann, 0.45 mm) and analyzed.

3. Results and discussion

3.1. Structural analysis

XRD patterns of prepared catalysts revealed the presence of single anatase phase in all case, except for 3%Li–TiO_2 **d** where 14.28 wt.% of rutile phase was also detected. The crystallinity level of each catalyst was found to be highly dependent on both the nature and the amount of alkaline used during the preparation. In particular, for the samples prepared by sol–gel route, the crystallinity level strongly depends on the amount of alkaline used. For lithium, it appears that crystallinity increases with increasing Li concentration. By contrast, no effect of sodium on the catalyst crystallinity was observed. Compared to lithium, in the case of potassium the opposite effect is observed. Indeed, the crystallinity of final products decreases with increasing K concentration.

The XRD pattern of 5%A–TiO_2 (with A: Li, Na, K) as prepared by sol–gel route are presented in Fig. 1. At first glance, if we compare the crystallinity of catalyst, it appears that the latter decreased from Li to K. The highest crystallinity is observed for Li-doped catalysts and the lower for K-doped catalysts. For catalysts prepared by impregnation technology (not presented in this report), pure anatase phase was observed with good crystallinity in all cases.

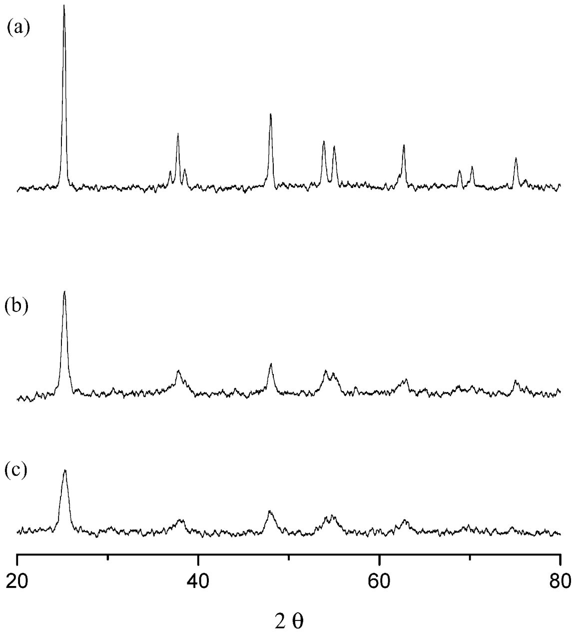

Fig. 1. XRD patterns of: (a) 5%Li–TiO_2 d; (b) 5%Na–TiO_2 d and (c) 5%K–TiO_2 d.

Table 1
Crystallite size and pH of zero charge of each catalyst

Catalysts	Crystallite size (nm)	pH_{pzc}
TiO_2 pure	20.40	6.6
1%Li–TiO_2 d	20.35	7.2
3%Li–TiO_2 d	24.67	7.4
5%Li–TiO_2 d	26.89	7.9
1%Li–TiO_2 i	17.47	7.00
3%Li–TiO_2 i	17.47	7.45
5%Li–TiO_2 i	17.47	7.7
1%Na–TiO_2 d	12.23	7
3%Na–TiO_2 d	12.23	7.15
5%Na–TiO_2 d	10.79	7.4
1%Na–TiO_2 i	17.47	7
1%K–TiO_2 d	12.23	7
3%K–TiO_2 d	10.19	7.05
5%K–TiO_2 d	6.79	7.2
1%K–TiO_2 i	17.47	7

The radius of Li^+, Na^+ and K^+ as a function of coordination number are Li^+(6): 0.7, Na^+ (6): 1.06 Å and K^+ (8, 12): 1.51 Å, 1.64 Å [17]. If we compare the latter radius with that of Ti^{4+} (6): 0.61 Å, it appears that only Li^+ can be introduced in TiO_2 lattice by Ti^{4+} substitution or by insertion as Li^0 into interstitial sites [10]. Na^+ and K^+ remain probably bounded with oxygen onto TiO_2 surface. Additionally, some secondary phases such as $K_2Ti_4O_9$ with perovskite structure and/or phases including potassium, probably in lamellar host may be formed [13]. In our case, we did not observe the formation of a secondary phase, probably due to their low concentrations and sensitivity of the instrument used.

Table 1 exhibits the crystallite sizes extracted from the XRD pattern and the pH of zero charge of the prepared catalysts. It is noted that all the catalysts are in nanoparticule form with sizes ranging from 6.79 to 26.89 nm. The lowest crystalline size is obtained for K-doped TiO_2 and the largest for Li-doped TiO_2.

3.2. Determination of pH_{pzc} of catalysts

Fig. 2 presents some evolution of the final pH obtained for several representative catalysts. The dashed lines refer to the case $pH_f = pH_i$. The pH of the point of zero charge (pH_{pzc}) was determined for all catalyst and listed in Table 1. Pure TiO_2 dispersed in the solutions at different pH was taken as a reference for comparison purposes.

For pure TiO_2 and for an initial pH below 5.5, final pH (pH_f) was found to be slightly greater than the initial one (pH_i), evidencing an acidity decrease of the solutions. The pH evolution can be explained by the presence of proton H^+ scavengers (basic sites) onto the TiO_2 surface. For $5.5 < pH_i < 7$, pH_f turns out to be constant that is to say independent from pH_i. In all cases, a value of pH 6.6 that is equal to pH_{pzc} is obtained. Indeed, the curve of pH_f as a function of pH_i crosses the line $pH_f = pH_i$ at pH_{pzc}. For $pH_i > 7$, pH_f was found to be slightly less than the pH_i, evidencing

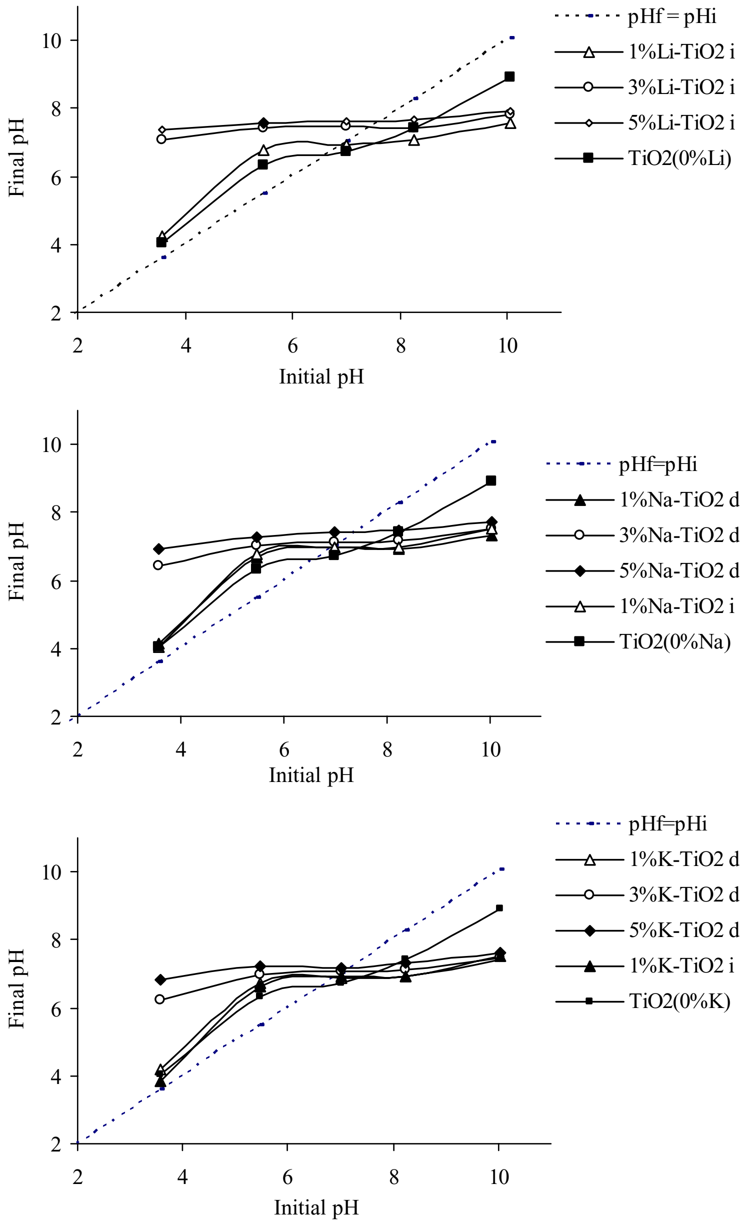

Fig. 2. pH drift method to obtain pH_{pzc} for x%A–TiO_2 (A: Li, Na, K).

a decrease of the basicity and meaning that a part of OH^- ions is neutralised by acidic site of pure TiO_2.

For 1%A–TiO_2 d–i, the pH evolution displays two features that are noteworthy. First, for $pH_i < 5.5$, the pH evolution exhibits the same trend as that of pure TiO_2 (described above), confirming a weak concentration of basic sites. For $pH_i > 5.5$, pH_f remains constant up to pH_i 10. This result reveals a high concentration of acidic sites in contrast with pure TiO_2.

For 3%A–TiO_2 and 5%A–TiO_2, the catalyst prescribes the pH_f in the whole studied pH_i domain, indicating that the surface is much more basic than that of 1%A–TiO_2. Therefore, increasing the alkaline concentrations above 1% creates *both* acidic and basic sites.

Possible explanations for the creation of basic and acid sites of the TiO_2 surface are given in the following. On the one hand, the increase acidic sites can be explained by the presence on the TiO_2 surface of alkaline known to present an acidic character. In the course of our experiments, we performed conductivity measurements of 20 MΩ bidistilled water containing dispersed catalysts. An increase in the water conductivity was then observed. A reasonable interpretation of this fact is that an amount of alkaline migrated from the TiO_2 surface to the solution in good agreement with the results reported by Yu and Zhao [18]. This phenomenon is responsible for the creation of basic sites at the surface of the catalyst according to the following reactions:

$$\text{–Ti–O–A} \rightarrow \text{–Ti–O}^- + \text{A}^+ \quad (\text{A : Li, Na, K}) \tag{1}$$

Therefore, doping TiO_2 with a well-controlled amount of alkaline could be an alternative way to improve both concentrations of acidic sites and basic sites. This latter fact presents several advantages in terms of adsorption properties and degradation selectivity.

The pH_{pzc} extracted from Fig. 2 are listed in Table 1. It is observed that pH_{pzc} increases significantly with alkaline concentration except for the case of potassium that shows a constant pH_{pzc} value.

3.3. Evaluation of the photocatalytic activity of doped-TiO_2

The photocatalytic activity of prepared catalysts was studied using three models of pollutants: Malachite green oxalate (MG), 4-hydroxybenzoic acid (4-HBZ) and benzamide (BZ). The efficiency of each catalyst is expressed in terms of half-life of the pollutant.

3.3.1. Effect of sodium

The effects of the amount of sodium on photocatalytic degradation of MG, 4-HBZ and BZ are presented in Fig. 3a–c. A significant deactivation of catalyst can be seen whatever the preparation method and Na concentration for MG and 4-HBZ. This deactivation is all the more significant for catalysts prepared by sol–gel route (direct method). These first results seem to confirm the observations made by Fernández et al. [13] in the case of supported photocatalysts.

For 4-hydroxybenzoic acid degradation, we observe that for 1%Na-doped TiO_2 prepared by impregnation technique, the photocatalytic efficiency is comparable to undoped catalysts (0%-TiO_2 and TiO_2-P25) whereas for other doped-catalysts one can appreciate a significant deactivation of TiO_2.

Photocatalytic degradation of Benzamide using pure TiO_2 prepared by sol–gel route is found less efficient than that of TiO_2-P25 (Fig. 3c). Nevertheless, Na improves the photocatalytic efficiency of TiO_2 as its concentration increases. The better catalyst is 1% Na-doped TiO_2 as prepared by impregnation method. The efficiency of the latter is even better than that of TiO_2-P25. These results do not agree with those reported in reference [13,14].

Several authors attribute deactivation of supported catalysts by the presence of Na into TiO_2 lattice [13,14]. Generally, two procedures of supported catalyst by sol–gel preparations are adopted:

(1) The glass is immersed into the gel solution at room temperature before being thermally treated;
(2) The gel is first calcinated until a suitable catalyst is obtained. The latter is then dispersed in acidic solutions in which a glass is immersed. Finally, the water is eliminated by evaporation and the glass is calcinated.

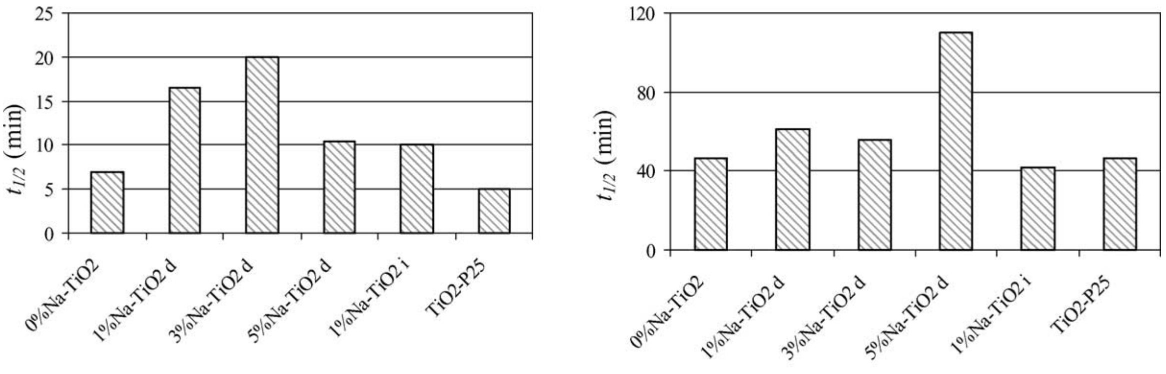

(a) **(MG)**

(b) **(4-HBZ)**

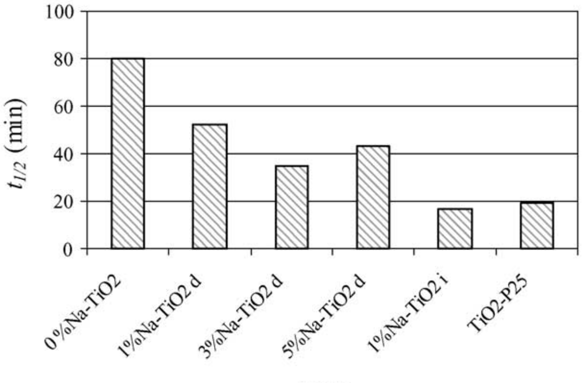

(c) **(BZ)**

Fig. 3. Half-life pollutant degradations as a function of Na doped TiO_2.

In all cases the contamination of catalysts by Na is attributed to the migration of Na from the bulk of the glass to the interface catalyst-glass during the calcination process above a certain temperature threshold depending on glass type.

In TiO_2 supported glass, the so-called poisoning effect is often attributed to Na. However, our results show that Na does not systematically decrease the photoactivity of TiO_2 but can improve, in some cases, TiO_2 efficiency. These contradictory effects seem to strongly depend on concentration, introduction method of Na into TiO_2 lattice and nature of pollutant to be degraded. Therefore, we can suggest that deactivation of supported TiO_2 could originate from the *combined effect* of several elements including Na, such as Ca, K and Mg, also present in the glass [18,19].

3.3.2. *Effect of potassium*

The effect of the amount of potassium on photocatalytic degradation of MG, 4-HBZ and BZ are presented in Fig. 4a–c, respectively. Compared to undoped TiO_2, K-doped TiO_2 gives rise to a remarkable increase in MG half-life time. The latter is enhanced when potassium concentration is increased. The deactivation of TiO_2 can be mainly explained by the poor crystallinity of catalyst (see Fig. 1). Often, when a dye is adsorbed onto TiO_2 surface, electrons are injected from its LUMO band to the conduction band of TiO_2 when the system is under illumination. This phenomenon induces an extension of the catalyst photoresponse and consequently, more radicals will be generated. Generally, this phenomenon is accompanied by an increase in the catalyst photoactivity as the adsorption of dyes increases. Unfortunately, this phenomenon does not occur in our situation, probably due to the high concentration of defect, each one acting as an electron–hole trapping system.

For the degradation of 4-HBZ (Fig. 4b), one notes that 1%K-doped TiO_2 as prepared by sol–gel method has no effect on the efficiency and, for even higher K concentrations (3 and 5%), desactivation of TiO_2 occurs. However, 1%K-doped TiO_2 as prepared by impregnation technique is found to be more efficient than undoped TiO_2. For benzamide (Fig. 4c), our results show that the photocatalytic efficiency of K-doped TiO_2 is much better than that of undoped TiO_2. Globally, the half-life of the pollutant is reduced by a factor of about 3–4. For the catalyst prepared by impregnation technique (1%K–TiO_2 i), the half-life of benzamide is even shorter and reaches that of TiO_2-P25. These results are in agreement with those of Morawski et al. [11]. These authors attribute the activation of catalyst to the more efficient electron–hole creation induced by the presence of potassium.

3.3.3. *Effect of lithium*

The effect of Li on the photocatalytic activity of TiO_2 for 4-HBZ degradation is shown in Fig. 5a and b. For the degradation 4-HBZ, the preparative method has a significant in-

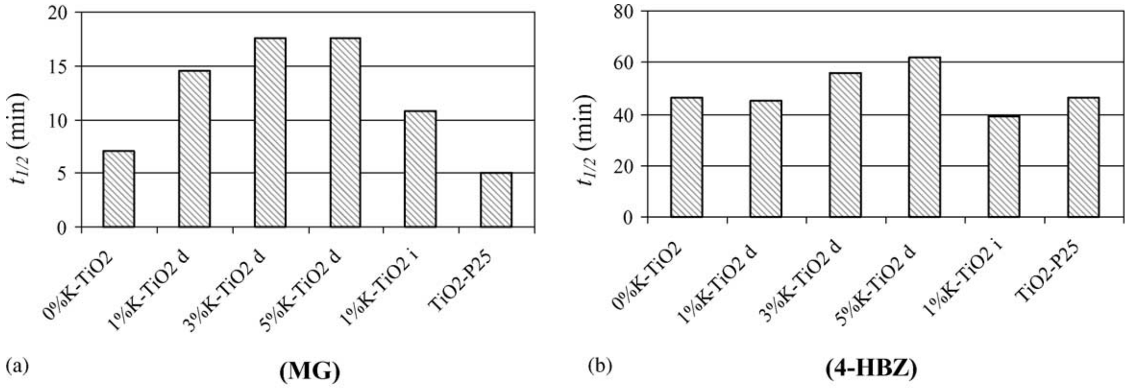

(a) **(MG)** (b) **(4-HBZ)**

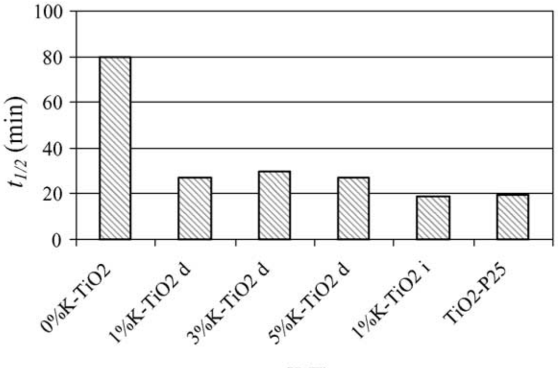

(c) **(BZ)**

Fig. 4. Half-life pollutant degradations as a function of Na doped TiO_2.

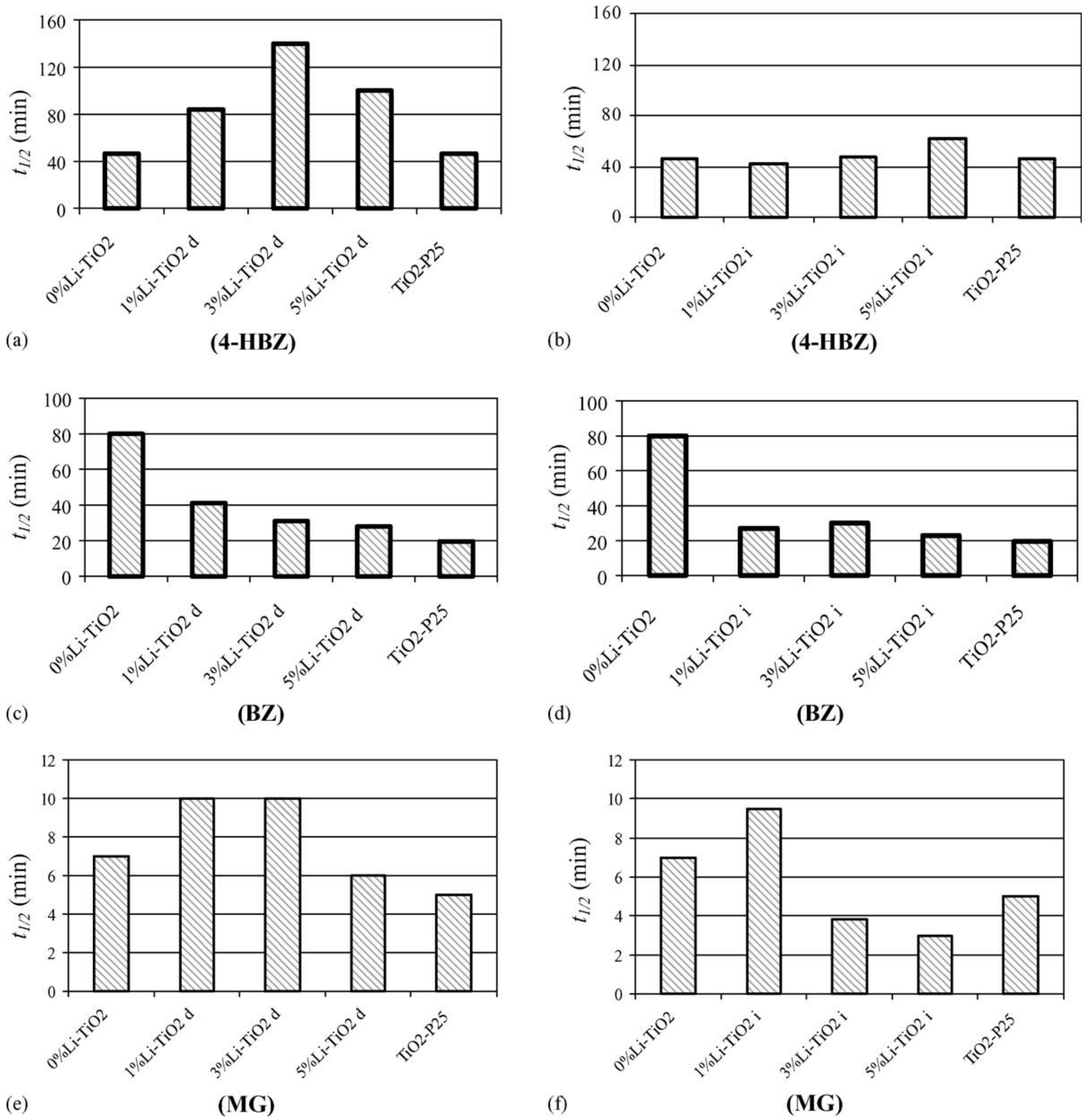

Fig. 5. Half-life of pollutant degradations as a function of Li doped TiO_2 (a–f).

fluence on the efficiency of the catalyst. When prepared with the sol–gel method, Li-doped TiO_2 is less efficient than the undoped reference. The half-life of 4-HBZ is at least twice that of the pure materials, whatever the studied doping levels. On the contrary, for the catalysts prepared by the impregnation method, an efficiency increase is observed for 1% Li-Doped TiO_2 in comparison to pure TiO_2. However, for higher Li doping levels, deactivation of the catalyst occurs and the half-life of increases with increasing Li percentage.

The effect of Li on the photocatalytic activity of TiO_2 for benzamide degradation is shown in Fig. 5c and d. At first glance, it appears that both Li concentration and preparation methods have little influence on the catalyst efficiency. The half-life of BZ is twice to four times shorter than that of undoped TiO_2. For 5%Li-doped TiO_2, the half-life of BZ is comparable to TiO_2-P25. Li improves the photocatalytic efficiency of TiO_2 and a dramatic activation of the catalyst is already observed for Li concentration as low as 1%. These results show that doping TiO_2 by Li can be considered as an alternative way to improve the efficiency of pure TiO_2 prepared by sol–gel route when applied to BZ degradation.

Fig. 5e and f show the variation of half-life MG as a function of Li concentration in the catalyst prepared by sol–gel route and impregnation technology, respectively. Depending on the prepration technique, Li-doped TiO_2 shows two contradictory behaviours. For the catalyst prepared by sol–gel route, the presence of Li reduces the catalyst photoactivity. Indeed, the photoactivity of doped catalyst is worse than undoped TiO_2, except for 5% Li-doped TiO_2 which is slightly better. For the catalyst prepared by impregnation technology, it is observed that above 1% Li, the catalyst shows a better efficiency than TiO_2-P25. In particular, for 5% Li-doped TiO_2, a half-life of the pollutant is found to be twice shorter than that observed for TiO_2-P25. This phenomenon can be attributed to a more favourable distribution of lithium on nanotitania, i.e. homogeneous distribution using sol–gel route and concentrated on the surface by impregnation method.

In order to explain why Li–TiO_2 prepared by impregnation technology is very efficient for the degradation of MG, a description of the charge transfer mechanisms is required. Doping TiO_2 with alkaline leads to the creation of negative charges at the catalyst surface according to Eq. (1) (Section 3.2). Furthermore, in the course of our experiments, we observed that the amount of adsorbed MG molecules increases with increasing Li concentration. Therefore, we can reasonably think that adsorption of MG that is a cationic molecule, is facilitated thanks to electrostatic interaction.

Under irradiation, adsorbed MG molecules on TiO_2 inject electrons into the conduction band of TiO_2 increasing the generation of electron by the catalyst. As a consequence, more oxygen peroxide radicals ($O_2^{-\bullet}$) are generated.

On the other hand, the presence of high Li concentration at TiO_2 surface gives rise to a negative potential shift of the conduction band edge [20]. Thus, the electric field developed across the depletion layer (*W*) increases. As a consequence, both electron injection (from the LUMO band of MG to the conduction band of Li–TiO_2) and charge separations in the semiconductors are improved.

As a conclusion, the 5% Li–TiO_2 prepared by impregnation technology is very efficient for MG degradation because of:

(i) the increased adsorption of the pollutant (compared to undoped TiO_2);
(ii) the TiO_2 spectral extension;
(iii) the active role of Li in the charge separation process;
(iv) the electron production improvement that increases the radical production.

4. Conclusion

Nanoparticles of alkaline-doped TiO_2 were prepared by sol–gel route and impregnation technology. XRD analysis showed that alkaline promotes anatase crystalline phase. pH drift method revealed that there is no significant difference between the catalyst prepared by sol–gel route and the catalyst prepared by impregnation technique for a given doping level. Additionally, it was observed that alkaline-doping increases acidic sites at low alkaline concentration (1 at.%) and basic sites at higher alkaline concentration.

Photocatalytic tests revealed that the efficiency of the catalyst is strongly dependent on the pollutant type, the alkaline type and its concentration. In general, catalysts prepared by impregnation technology were found to be more efficient than those prepared by sol–gel route. For MG degradation, the best photoactivity was obtained for 5% Li-doped TiO_2 *i*. The latter showed an efficiency that was even better than TiO_2-P25. This effect was attributed to the presence of Li at TiO_2 surface that improves electron transfer efficiency from the LUMO band of MG to the conduction band of TiO_2, consequently increasing the amount of produced radicals.

In the case of 4-HBZ degradation, catalyst prepared by impregnation technology and containing (1 at.%) of alkaline were found to be more efficient than commercial catalyst TiO_2-P25.

When BZ is used as a pollutant, pure TiO_2 prepared by sol–gel route usually exhibits a lower efficiency than that of commercial TiO_2-P25. When alkaline-doped TiO_2 is prepared by impregnation method, a small concentration of alkaline activates the catalyst. In particular, for Na concentration as low as 1%, Na-doped TiO_2 is even better than TiO_2-P25. From these results, one can conclude that in small concentrations, alkaline improves TiO_2 efficiency.

Another important conclusion that we can draw from our results is the effect of Na on TiO_2 photoactivity that is strongly dependent on its concentration, the doping method and the type of substrate to be removed. It is then clear that sodium can activate TiO_2. Therefore, the deactivation of supported catalyst, also called "poisoning", cannot be systematically attributed to the presence of Na as claimed by several authors. We suggest that the main reason for "poisoning" could be the *associated* effect of several elements present in the support.

References

[1] M. Schiavello (Ed.), Heterogeneous Photocatalysis, Wiley, New York, 1997.
[2] D. Bahnemann, in: P. Boule (Ed.), Handbook of Environmental Photochemistry, Springer, Verlag, 1999, 285 p.
[3] D. Robert (Ed.), Industrial and Environmental Applications of Photocatalysis (special issue), Int. J. Photoenergy, vol. 5, issues 2–3 (2003).
[4] P. Pichat, in: G. Ert, H. Knözinger, J. Weitkamp (Eds.), Handbook of Heterogeneous Photocatalysis, VCH, Weiheim, 1997, p. 2111.
[5] D.F. Ollis, H. Al-Ekabi (Eds.), Photocatalytic Purification and Treatment of Water and Air, Elsevier, Amsterdam, 1993.
[6] D. Robert, J. Lede, J.V. Weber (Eds.), Special Issue in Entropie, No. 228 (2000).
[7] S. Malato, J. Blanco, A. Vidal, C. Richter, Appl. Catal. B: Environ. 37 (2002) 1.
[8] K. Pirkanniemi, M. Sillanpää, Chemosphere 48/10 (2002) 1047.
[9] V. Brezová, A. Blažková, L. Karpinský, J. Grošková, B. Havlínová, V. Jorík, M. Èeppan, J. Photochem. Photobiol. A: Chem. 109 (1997) 177.
[10] T. López, J. Hernandez-Ventura, R. Gómez, F. Tzompantzi, E. Sánchez, X. Bokhimi, A. García, J. Mol. Catal. A: Chem. 167 (2001) 101.
[11] A.W. Morawski, J. Grzechulska, K. Kalucki, J. Phys. Chem. Solids 57 (1996) 1011.
[12] J. Grzechulska, M. Hamerski, A.W. Morawski, Wat. Res. 34 (2000) 1638.
[13] A. Fernández, G. Lassaletta, V.M. Jiménez, A. Justo, A.R. González-Elipe, J.-M. Herrmann, H. Tahiri, Y. Ait-Ichou, Appl. Catal. B: Environ. 7 (1995) 49.

[14] Y. Paz, Z. Luo, L. Rabenberg, A. Heller, J. Mater. Res. 10 (1995) 2842.
[15] Y. Bessekhouad, D. Robert, J.V. Weber, J. Photochem. Photobiol. A: Chem. 157 (2003) 47.
[16] G. Newcombe, R. Hayes, M. Dribas, Colloids Surf. A 78 (1993) 65.
[17] R.D. Shannon, Acta Crystallography A32 (1976) 751.
[18] J. Yu, X. Zhao, Mater. Res. Bull. 36 (2001) 97.
[19] M. Karches, M. Morstein, P.R. von Rohr, R.L. Pozzo, J.L. Giombi, M.A. Baltanás, Catal. Today 72 (2002) 267.
[20] Y. Liu, A. Hagfeld, X.R. Xiao, S.E. Lindquist, Sol. Energy Mater. Sol. Cells 55 (1998) 267.